Figure 13. The phenomenon observe where about 30-cm thick scum is accumulated at tank

NONLINEAR DYNAMIC ANALYSIS OF LAMINATED COMPOSITE PLATES UNDER IN-PLANE COMPRESSIVE LOADS

Dr. Husain M. Husain
Professor
in Civil Engineering,
University of Tekrit

Dr. Nameer A. Alwash
Professor
in Civil Engineering,
University of Babylon

Dr. Haider K. Ammash
Lecturer.
in Civil Engineering,
University of Al-Qadisyia

Abstract

A nonlinear finite element method is adopted for the large displacement elastic-plastic dynamic analysis of anisotropic plates under in-plane compressive loads. The analysis is based on the two-dimensional layered approach with classical and higher order shear deformation theory with five, seven, and nine degrees of freedom per node, nine-node Lagrangian isoparametric quadrilateral elements are used for the discretization of the laminated plates. Both consistent and lumped mass matrices are used in the present study. Damping property is considered by using Rayleigh type damping which is linearly related to the mass and the stiffness matrices. **Newmark** integration method is used for solving the dynamic equilibrium equations. The effects of initial imperfection, orthotropy of individual layers, fiber's orientation angle, type of loading, damping factor, and fiber waviness on the large displacement elastic-plastic dynamic analysis are considered. The conclusion it is shown that the antisymmetric cross-ply laminated plate has a damping rate faster than the symmetric cross-ply laminated plate and if damping is considered and if the response of the plate shows no oscillation about the static deflection position, it means that the damping factor is below the critical damping factor.

التحليل الديناميكي اللاخطي للصفائح غير متماثلة الخواص تحت حمل ضغط في المستوي

د. حسين محمد حسين أستاذ/جامعة تكريت
د. نمير عبد الأمير علوش أستاذ مساعد/جامعة بابل
د.حيدر كاظم عماش مدرس/جامعة القادسية

الخلاصة
تم تقديم طريقة العناصر المحددة اللاخطية لتحليل الازاحة الكبيره المرن-اللدن الاستاتيكي للصفائح غير متماثلة الخواص تحت حمل ضغط في المستوي. تبنت هذه الدراسة طريقة الطبقة ثنائي البعد(two-dimensional layered approach) واعتمدت نظرية التشوهات القصية الكلاسيكية وذات المرتبة العليا (classical and higher order shear deformation theory) مع خمس،وسبع وتسع درجات حرية لكل عقدة، تم توظيف عنصر لاكرانج (Lagrangian) ذي العقد التسع لتمثيل الصفائح الطبقية. تم استعمال مصفوفة الكتلة المتوافقة والكتلة المتكومة في هذه الدراسة. كذلك، تم استخدام مصفوفة إخماد رايلي (Rayleigh type damping matrix) للتعبير عن خواص الاخماد. تم استخدام طريقتين (Newmark integration method) و(harmonic acceleration method) لحل معادلة التوازن الديناميكي. وقد

أُخذ بنظر الاعتبار تأثير التقوس الابتدائي وخطوة الوقت وظروف الاسناد وتعامد الخواص للطبقات المنفردة وزاوية تدوير الالياف ونوع الحمل وقيمة الحمل ومعامل التخميد وتموج الالياف على تحليل الازاحة الكبيره انالصفائح الطبقية المتعامدة غير المرن-اللدن الديناميكي. ا من النتائج المستحصلة، يمكن ملاحظة) تمتلك معدل تخميد اعلى من معدل تخميد الصفائح الطبقية المتعامدة antisymmetric cross-plyتناظرياً( )،واذا اخذ التخميد بنظر الاعتبار وتصرف الصفيحة اظهر عدم اي تذبذب symmetric cross-plyتناظرياً (حول موضع الهطول الاستاتيكي، فهذا يعني أن معامل التخميد تحت معامل التخميد الحرج.

Notations

Symbol	Description
a, b	Plate dimensions in **x** and **y**-directions, respectively.
[B]	Strain-nodal displacement matrix.
D	Flexural rigidity = $Et^3/12(1-v^2)$.
$\{d\}$	Displacement vector.
$\{\dot{d}\}$	Velocity vector.
$\{\ddot{d}\}$	Acceleration vector.
E_i	Modulus of elasticity in i-direction.
E_f	Modulus of elasticity of fiber.
E_m	Modulus of elasticity of matrix.
$\{F\}$	External load vector.
F	Yield function.

$\{F(t)\}$	Dynamic external force vector.
G	Shear modulus.
h_L-h_{L-1}	Distance from plate middle surface to the upper and lower surface of L^{th} lamina.
h	Plate thickness.
$[K_o]$	Constant linear elastic stiffness matrix
$[K_L]$	Initial or large displacement matrix
$[K_\sigma]$	Initial stress stiffness matrix
$[K_T]_0$	Tangent stiffness matrix.
M_x, M_y, M_{xy}	Bending and twisting moments (per unit width) (on **yz**, **xz**, and both **yz** and **xz**-sections).
M_x^*, M_y^*, M_{xy}^*	Higher order bending and twisting moments (per unit width) (on **yz**, **xz**, and both **yz** and **xz**-sections).
N_x, N_y, N_{xy}	In-plane stress resultants (per unit width) (on **yz**, **xz**, and both **yz** and **xz**-sections).
N_x^*, N_y^*, N_{xy}^*	Higher order in-plane stress resultants (per unit width) (on **yz**, **xz**, and both **yz** and **xz**-sections).
$\mathbf{P_x}$	In-plane applied load in **x**-direction.
Q_{ij}	Element of elasticity matrix with respect to Cartesian coordinate system
Q_x, Q_y	Transverse shearing forces (per unit width) (on **yz** and **xz**-sections).
Q	Uniformly distributed load (per unit area).
$\{\Delta R\}$	Residual load vector.
[T]	Transformation matrix.
u,v,w	Displacement components in **x**,**y** and **z** direction, respectively.
w_o	Amplitude of initial imperfection.
x,y,z	Coordinates.
γ_{ij}^o	Shear strain in ij-plane at middle surface.
γ_{ij}^{o*}	Higher order shear strain in ij-plane at middle surface.
$\{\varepsilon\}$	Strain vector.
$\{\varepsilon_o\}$	Middle surface strain vector.
ε_i	Normal strain in i-direction.
ε_i^o	Normal strain in i-direction at middle surface.
ε_i^{o*}	Higher order normal strain in i-direction at middle surface.
ξ, η	Curvilinear coordinates system.
θ	Fiber's orientation angle.
θ_x, θ_y	Rotations of transverse normals in the (**xz**) and (**yz**) planes.
θ_x^*, θ_y^*	Higher order rotations of transverse normals in the (**xz**) and (**yz**) planes.
κ_i^o	Bending curvature in i-plane at middle surface.
κ_{ij}^o	Bending curvature in ij-plane at middle surface.
κ_i^{o*}	Higher order bending curvature in i-plane at middle surface.
κ_{ij}^{o*}	Higher order bending curvature in ij-plane at middle surface.
ν_i	Poisson's ratio in i-direction.

$\{\sigma\}$ Stress vector at sampling point.

σ_o Yield stress of steel

Introduction

Certain civil engineering structures are designed to carry their own dead load plus superimposed loads which are immovable and unvarying with time, that is, superimposed static loads. In such cases, the stress analysis involves only principles of statics. More often the design of a civil engineering structure involves not only static loads but also superimposed loads which are either moving or movable and may vary with time as in superimposed dynamic loads. In such cases, the stress analysis properly should involve principles of dynamics to determine the effect of dynamic loading.

However, in many of these cases, experience has shown that the dynamic effect makes a minor contribution to the total load which must be provided for the design and therefore the dynamic effect need not be evaluated precisely. In such cases, the dynamic effect may be handled by the use of an equivalent static load, or by an impact factor or by a modification of the factor of safety.

There have been a number of developments which have led to growing interest in a more precise evaluation of the effects produced by the dynamic portion of the loading. Among these are the imposition of more severe live load conditions (that is, machinery and vehicles moving at high speeds), the construction of high towers and long bridges involving more severe and important wind-loading conditions, the necessity of developing blast resistant constructions, and the desire to improve earthquake resistance of constructions. These are some aspects where it may be necessary to consider more precisely the response produced by dynamic loading.

The ability of thin-walled structures to absorb the energy of dynamic transient loading has led to its utilization for several classes of important structures, such as aerodynamic structures, power plant structure, bridge structures, etc. These types of structures are designed under these loads to maintain the overall structural integrity with irreversible deformation analysis. **Weller**, **et al.** [**1989**] [(21)] used the ADINA computer code for determining the dynamic load amplification factor (DLF) for beams and plates under in-plane impact loads. Good agreement was found in comparisons with self-developed finite difference computer codes and available experimental results. Though the problem that had been studied was of a wave propagation nature, a relatively small number of time steps were found to be enough to describe the phenomenon quite accurately. This can be attributed to the relatively short time duration of the applied loading (around the natural period of the structure). They observed that the DLF was usually larger than unity, both for beams and plates. In the presence of certain values of relatively large initial geometric imperfections and combined with periods of the applied load which were close to the first period of natural lateral vibrations of either the beam or the plate, DLF would be smaller than unity. In [**1993**][(14)], **Kommineni** and **Kant** presented a C^o-continuous finite element formulation of a higher order displacement theory for predicting linear and geometrically nonlinear behavior in the sense of von-Karman transient response of composite and sandwich plates. The displacement model accounts for nonlinear cubic variation of the tangential displacement components through the thickness of the laminated plate and the theory requires no shear correction coefficients. The

parametric effects of the time step, finite element mesh, lamination scheme, and orthotropy on the linear and geometrically nonlinear responses were investigated. Their numerical results for central transverse deflection, stress, and stress resultant were presented for rectangular composite and sandwich plates under various boundary conditions and loadings. The conclusion of their study was that the refined shear deformation theory is essential for predicting accurate responses of layered composite and sandwich laminates. **Tao, et al.** [**2004**][19] presented a simple solution of the dynamic buckling of stiffened plates under impact loading. Based on large deflection theory, a discretely stiffened plate model had been used. The tangential stresses of stiffeners and their in-plane displacements were neglected. The motion equations of stiffened plates were obtained by using Lagrange-Hamilton's principle. The deflection of the plate was expressed as Fourier series, and by using Galerkin method the discrete equations were solved by Runge-Kutta method. Their results were in excellent agreement with the finite element method. They observed that the Budiansky-Roth criterion was partially applicable for detecting the dynamic buckling of a stiffened plate. The conclusion of their study was that an appropriate shape of initial imperfection would avoid local buckling of the structure under impact load. From the preceding review of literature, it is clear that there is no study which considers the nonlinear dynamic analysis of isolated laminated plate under axial compression load by taking into account the effect of damping, type of loading, and type of fiber (straight or wavy). There is also a little amount of literature that takes into account the higher order displacement model of nine degrees of freedom per node with different types of lamination.

Laminated Plate Theories

A laminated plate is a series of laminas bonded together to act as an integral structural element. Thus, a laminate is not a material but instead a structural element with essential features of both material properties and geometry. The stiffness and strength of such a composite material with structural configuration are obtained from the properties of the constituent laminas, and thus the macromechanical behavior of a laminate is the main topic of this section. The lamination so described can be considered as a single layer with "rule of mixtures" representation of the interaction between the multiple laminas in a plate or shell [**Jones, 1999**][10].

There are two categories of theories, equivalent single layer and three dimensional elasticity theories. In the first category, the material properties of the constituent layer are smeared to form a hypothetical single layer whose properties are equivalent to through thickness integrated sum of its constituents, and this category contains classical lamination theory, first order shear deformation theory, and higher

order shear deformation theory. The higher order shear deformation theories are more efficient to represent the transverse shear deformation, through-thickness displacement and strains. The assumption of a higher order plate theory can also be used within the equivalent layer formulation [**Jones, 1999**][10]. The strain expressions derived from the displacement field were considered by **[Ali, 2004**][3] with nine degrees of freedom per node as follows:

$$\begin{aligned} u(x,y,z,t) &= u_o(x,y,t) + z\theta_x(x,y,t) + z^2 u_o^*(x,y,t) + z^3\theta_x^*(x,y,t) \\ v(x,y,z,t) &= v_o(x,y,t) + z\theta_y(x,y,t) + z^2 v_o^*(x,y,t) + z^3\theta_y^*(x,y,t) \\ w(x,y,z,t) &= w_o(x,y,t) \end{aligned} \quad \textbf{(1)}$$

in which the parameters (u, v, w, θ_x, θ_y, θ_x^*, and θ_y^*) are defined previously, u_o^*, and v_o^* are the corresponding higher order terms in Taylor's series expression and they are also defined at the middle plane. The strain-displacement relations after differentiating Equation (1) are:

$$\begin{aligned} \varepsilon_x &= \frac{\partial u}{\partial x} = \varepsilon_x^o + z\kappa_x + z^2\varepsilon_x^{o^*} + z^3\kappa_x^* \\ \varepsilon_y &= \frac{\partial v}{\partial y} = \varepsilon_y^o + z\kappa_y + z^2\varepsilon_y^{o^*} + z^3\kappa_y^* \\ \gamma_{xy} &= \frac{\partial u}{\partial y} + \frac{\partial v}{\partial x} = \gamma_{xy}^o + z\kappa_{xy} + z^2\gamma_{xy}^{o^*} + z^3\kappa_{xy}^* \\ \gamma_{xz} &= \frac{\partial u}{\partial z} + \frac{\partial w}{\partial x} = \varphi_x + z\gamma_{xz}^o + z^2\varphi_x^* \\ \gamma_{yz} &= \frac{\partial v}{\partial z} + \frac{\partial w}{\partial y} = \varphi_y + z\gamma_{yz}^o + z^2\varphi_y^* \end{aligned} \quad \textbf{(2)}$$

where

$$\begin{aligned} &\varepsilon_x^o = \frac{\partial u_o}{\partial x},\ \varepsilon_y^o = \frac{\partial v_o}{\partial y},\ \gamma_{xy}^o = \frac{\partial u_o}{\partial y} + \frac{\partial v_o}{\partial x} \\ &\kappa_x = \frac{\partial \theta_x}{\partial x},\ \kappa_y = \frac{\partial \theta_y}{\partial y},\ \kappa_{xy} = \frac{\partial \theta_x}{\partial y} + \frac{\partial \theta_y}{\partial x} \\ &\varphi_x = \theta_x + \frac{\partial w_o}{\partial x} \\ &\varphi_y = \theta_y + \frac{\partial w_o}{\partial y} \\ &\varepsilon_x^{o^*} = \frac{\partial u_o^*}{\partial x},\ \varepsilon_y^{o^*} = \frac{\partial v_o^*}{\partial y},\ \gamma_{xy}^{o^*} = \frac{\partial u_o^*}{\partial y} + \frac{\partial v_o^*}{\partial x} \\ &\gamma_{xz}^{o^*} = 2u_o^* \\ &\gamma_{yz}^{o^*} = 2v_o^* \end{aligned} \quad \textbf{(3)}$$

Also, all the strains above are defined in the middle-plane of the laminate. By substitution from Equation (3) into the stress-strain relations given by the following Equation:

$$\begin{bmatrix}\sigma_x\\ \sigma_y\\ \tau_{xy}\\ \tau_{xz}\\ \tau_{yz}\end{bmatrix}=\begin{bmatrix}Q_{11} & Q_{12} & Q_{16} & 0 & 0\\ Q_{12} & Q_{22} & Q_{26} & 0 & 0\\ Q_{16} & Q_{26} & Q_{66} & 0 & 0\\ 0 & 0 & 0 & Q_{55} & Q_{45}\\ 0 & 0 & 0 & Q_{45} & Q_{44}\end{bmatrix}\begin{bmatrix}\varepsilon_x\\ \varepsilon_y\\ \gamma_{xy}\\ \gamma_{xz}\\ \gamma_{yz}\end{bmatrix} \qquad \textbf{(4)}$$

After complete integration, the stress-resultant/strain relations of the laminate are as follows:

$$\begin{bmatrix}N_x\\ N_y\\ N_{xy}\\ N_x^*\\ N_y^*\\ N_{xy}^*\\ M_x\\ M_y\\ M_{xy}\\ M_x^*\\ M_y^*\\ M_{xy}^*\end{bmatrix}=\begin{bmatrix}A_{11} & A_{12} & A_{16} & D_{11} & D_{12} & D_{16} & B_{11} & B_{12} & B_{16} & E_{11} & E_{12} & E_{16}\\ A_{12} & A_{22} & A_{26} & D_{12} & D_{22} & D_{26} & B_{12} & B_{22} & B_{26} & E_{12} & E_{22} & E_{26}\\ A_{16} & A_{26} & A_{66} & D_{16} & D_{26} & D_{66} & B_{16} & B_{26} & B_{66} & E_{16} & E_{26} & E_{66}\\ D_{11} & D_{12} & D_{16} & F_{11} & F_{12} & F_{16} & E_{11} & E_{12} & E_{16} & G_{11} & G_{12} & G_{16}\\ D_{12} & D_{22} & D_{26} & F_{12} & F_{22} & F_{26} & E_{12} & E_{22} & E_{26} & G_{12} & G_{22} & G_{26}\\ D_{16} & D_{26} & D_{66} & F_{16} & F_{26} & F_{66} & E_{16} & E_{26} & E_{66} & G_{16} & G_{26} & G_{66}\\ B_{12} & B_{12} & B_{16} & E_{11} & E_{12} & E_{16} & D_{11} & D_{12} & D_{16} & F_{11} & F_{12} & F_{16}\\ B_{12} & B_{22} & B_{26} & E_{12} & E_{22} & E_{26} & D_{12} & D_{22} & D_{26} & F_{12} & F_{22} & F_{26}\\ B_{16} & B_{26} & B_{66} & E_{16} & E_{26} & E_{66} & D_{16} & D_{26} & D_{66} & F_{16} & F_{26} & F_{66}\\ E_{11} & E_{12} & E_{16} & G_{11} & G_{12} & G_{16} & F_{11} & F_{12} & F_{16} & H_{11} & H_{12} & H_{16}\\ E_{12} & E_{22} & E_{26} & G_{12} & G_{22} & G_{26} & F_{12} & F_{22} & F_{26} & H_{12} & H_{22} & H_{26}\\ E_{16} & E_{26} & E_{66} & G_{16} & G_{26} & G_{66} & F_{16} & F_{26} & F_{66} & H_{16} & H_{26} & H_{66}\end{bmatrix}\begin{bmatrix}\varepsilon_x^o\\ \varepsilon_y^o\\ \gamma_{xy}^o\\ \varepsilon_x^{o*}\\ \varepsilon_y^{o*}\\ \gamma_{xy}^{o*}\\ \kappa_x\\ \kappa_y\\ \kappa_{xy}\\ \kappa_x^*\\ \kappa_y^*\\ \kappa_{xy}^*\end{bmatrix} \qquad \textbf{(5)}$$

and,

$$\begin{bmatrix}Q_x\\ Q_y\\ S_x\\ S_y\\ Q_x^*\\ Q_y^*\end{bmatrix}=\begin{bmatrix}A_{55} & A_{45} & B_{55} & B_{45} & D_{55} & D_{45}\\ A_{45} & A_{44} & B_{45} & B_{44} & D_{45} & D_{44}\\ B_{55} & B_{45} & D_{55} & D_{45} & E_{55} & E_{45}\\ B_{45} & B_{44} & D_{45} & D_{44} & E_{45} & E_{44}\\ D_{55} & D_{45} & E_{55} & E_{45} & F_{55} & F_{45}\\ D_{45} & D_{44} & E_{45} & E_{44} & F_{45} & F_{44}\end{bmatrix}\begin{bmatrix}\varphi_x\\ \varphi_y\\ \gamma_{xz}^{o*}\\ \gamma_{yz}^{o*}\\ \varphi_x^*\\ \varphi_y^*\end{bmatrix} \qquad \textbf{(6)}$$

All coefficients in ***A***, ***B***, ***D***, ***E***, ***F***, ***G***, and ***H*** groups are defined as follows:

$$A_{ij}=\sum_{L=1}^{NL}Q_{ij}(h_L-h_{L-1}) \qquad i,j = 1, 2, 6 \text{ or } i,j = 4, 5 \qquad \textbf{(7 a)}$$

$$B_{ij}=(1/2)\sum_{L=1}^{NL}Q_{ij}(h_L^2-h_{L-1}^2) \qquad i,j = 1, 2, 6 \text{ or } i,j = 4, 5 \qquad \textbf{(7 b)}$$

$$D_{ij}=(1/3)\sum_{L=1}^{NL}Q_{ij}(h_L^3-h_{L-1}^3) \qquad i,j = 1, 2, 6 \text{ or } i,j = 4, 5 \qquad \textbf{(7 c)}$$

$$E_{ij}=(1/4)\sum_{L=1}^{NL}Q_{ij}(h_L^4-h_{L-1}^4) \qquad i,j = 1, 2, 6 \text{ or } i,j = 4, 5 \qquad \textbf{(7 d)}$$

$$F_{ij}=(1/5)\sum_{L=1}^{NL}Q_{ij}(h_L^5-h_{L-1}^5) \qquad i,j = 1, 2, 6 \text{ or } i,j = 4, 5 \qquad \textbf{(7 e)}$$

$$G_{ij}=(1/6)\sum_{L=1}^{NL}Q_{ij}(h_L^6-h_{L-1}^6) \qquad i,j = 1, 2, 6 \qquad \textbf{(7 f)}$$

$$i,j = 1, 2, 6 \qquad \textbf{(7 g)}$$

$$H_{ij} = (1/7)\sum_{L=1}^{NL} Q_{ij}\,(h_L^7 - h_{L-1}^7)$$

The present study explores the idea of tailoring the profile of reinforcing fibers to improve the buckling strength of composite plates. This study investigates the effect of waviness of fibers on the dynamic buckling curves, as shown in Figure (4), and this waviness is of the form:

$$y(x) = \alpha \sin\left(\frac{k\pi x}{a}\right) \qquad (8)$$

such that the angle of fiber orientation θ varies along the longitudinal x-axis as:

$$\tan(\theta) = \frac{dy}{dx} = \frac{\alpha k\pi}{a}.\cos\left(\frac{k\pi x}{a}\right) = \Delta k\pi.\cos(k\pi\bar{x}) \qquad (9)$$

where a = plate length; k= number of half sine waves; and α= wave amplitude. Two normalized variables, $\Delta=\alpha/a$ and $\bar{x} = x/a$, are introduced.

The main objective is to study the effect of fiber waviness, characterized by k and Δ, on the static and dynamic buckling behavior of composite laminates. The fiber can also be rotated in any direction with the x-axis, as shown in Figure (3), by using the following expression:

$$x_n = x\cos(\beta) + y\sin(\beta) \qquad (10)$$

where x_n represent the x-coordinate for a rotated fiber, and β is the angle of the waviness fiber.

The angle of fiber orientation in Equation (9) is variable with x-coordinate and instead of the constant angle used for straight fibers.

Figure (4) shows the principal material directions aligned with the lamina axes by angle (β).

Dynamic Equilibrium Equation

The dynamic equilibrium Equations are obtained by using the principle of virtual work which states that for any arbitrary kinematically consistent set of displacements, the internal virtual work done by stresses through virtual strains must be equal to that done by the external forces irrespective of the material behavior as [**Cook**, **1995**][8]:

$$\int_v (d\varepsilon)^T \sigma\, dv = \int_{s_t} (du)^T P_t\, ds + \int_v (du)^T (P_b - \rho\ddot{u} - C\dot{u})dv \qquad (11)$$

where du is a vector of virtual displacements, $d\varepsilon$ is the vector of associated virtual strains and σ is the vector of actual stresses. The term P_t is a vector of surface tractions acting on the portion s_t of the boundary S. Vectors $P_b, \rho\ddot{u}$ and $C\dot{u}$ are the body, inertial and damping forces respectively. The symbol ($\dot{}$) denotes differentiation with respect to time. ρ is the mass density and C is the damping parameter.

For the finite element representation, the displacements, velocities and accelerations $u, \dot{u}$ and $\ddot{u}$ can be defined in terms of the nodal variables $d, \dot{d}$ and $\ddot{d}$ by the expressions

$$u = \sum_{i=1}^{m} N_i(\xi,\eta)\, d_i = Nd \qquad du = N\,\delta d \qquad (12)$$

$$\dot{u} = \sum_{i=1}^{m} N_i(\xi,\eta)\, \dot{d}_i = N\,\dot{d} \qquad (13)$$

$$\ddot{u} = \sum_{i=1}^{m} N_i(\xi,\eta)\, \ddot{d}_i = N\,\ddot{d} \qquad (14)$$

where $u = \sum_{i=1}^{m} N_i(\xi,\eta)\, d_i = Nd$, N_i is the shape functions for i node, and m is the number of nodes.

With standard strain-nodal displacement matrix $[B]$, the virtual strain vector can be related to the nodal displacements as:

$$d\varepsilon = \sum_{i=1}^{m} [B]_i\, \delta d_i = [B]\delta d \qquad (15)$$

Upon substitution of Equations (12-15) into Equation (11) then:

$$\delta d^T \left[[M]\ddot{d} + [C]\dot{d} + [K]d \right] = \delta d^T \{ f_e(t) \} \qquad (16)$$

in which the mass matrix $[M]$, the damping matrix $[C]$, the stiffness matrix $[K]$ and the external applied vector $\{f_e(t)\}$ have the following element contributions:

$$[M_e] = \int_{Ve} N^T \rho\, N\, dV \qquad (17)$$

$$[C_e] = \int_{Ve} N^T C\, N\, dV \qquad (18)$$

$$[K_e] = \int_{Ve} [B]^T [D][B]\, dV \qquad (19)$$

$$f_e(t) = \int_{se} N^T P_t\, ds + \int_{Ve} N P_b\, dV \qquad (20)$$

where s_e and V_e denote the surface and volume of the element under consideration. As δd^T is arbitrary, then Equation (16) may be written as:

$$[M]\{\ddot{d}\} + [C]\{\dot{d}\} + [K]\{d\} = \{ f_e(t) \} \qquad (21)$$

Equation (21) is the dynamic equilibrium Equation for a single or multi-degree of freedom system.

Tangent Stiffness Matrix

The tangent stiffness matrix can be written as:

$$[K_T]=[K_o]+[K_L]+[K_\sigma] \quad \textbf{(22)}$$

where $[K_o]$ is the constant linear elastic stiffness matrix and can be written as:

$$[K_o]=\int_A [B_o]^T [D][B_o]dA \quad \textbf{(23)}$$

$[K_L]$ is the initial or large displacement matrix which is quadratically dependent upon displacement $\boldsymbol{u}$, and can be written as:

$$[K_L]=\int_A [B_o]^T [D][B_L]dA+\int_A [B_L]^T [D][B_L]dA+\int_A [B_L]^T [D][B_o]dA \quad \textbf{(24)}$$

Finally $[K_\sigma]$ is the initial stress stiffness matrix and then:

$$d[B_L]^T=\begin{bmatrix} 0 & 0 \\ d[B_L^b]^T & 0 \end{bmatrix} \quad \textbf{(25)}$$

Thus,

$$[K_\sigma]=\int_A \begin{bmatrix} 0 & 0 \\ [G]^T d[A]^T & 0 \end{bmatrix} \begin{Bmatrix} N_x \\ N_y \\ N_{xy} \\ M_x \\ M_y \\ M_{xy} \end{Bmatrix} \quad \textbf{(26)}$$

However, using the mathematical properties of the matrix **[*A*]**, this matrix can be written as:

$$d[A]^T \begin{Bmatrix} N_x \\ N_y \\ N_{xy} \end{Bmatrix}=\begin{bmatrix} N_x & N_{xy} \\ N_{xy} & N_y \end{bmatrix}[G]da \quad \textbf{(27)}$$

and finally one can obtain

$$[K_\sigma]=\begin{bmatrix} 0 & 0 \\ 0 & [K_\sigma^b] \end{bmatrix} \quad \textbf{(28)}$$

Thus,

$$[K_\sigma]=\int_A [G]^T \begin{bmatrix} N_x & N_{xy} \\ N_{xy} & N_y \end{bmatrix}[G]da \quad \textbf{(29)}$$

Formulation of Element Mass Matrix

The kinetic energy of the element (e) can be expressed as follows:

$$TI^e = \frac{1}{2}\int_A \{\dot{d}\}^T [m]\{\dot{d}\} dA \quad \textbf{(30)}$$

The velocity vector within an element is discretized such that:

$$\{\dot{d}\} = \sum_{i=1}^{NN} N_i \{\dot{d}\}, \text{ NN: number of nodes.} \quad \textbf{(31)}$$

By substituting Equation (31) into Equation (30), one gets:

$$TI^e = \frac{1}{2}\sum_{i=1}^{NN} \{\dot{d}\}^T \int_A N_i^T [m] N_i \, dA \{\dot{d}\} \quad \textbf{(32)}$$

Thus,

$$[M]^e = \int_A [N]^T [m][N] dA = \int_{-1}^{1}\int_{-1}^{1} [N]^T [M][N] |J| \, d\xi \, d\eta \quad \textbf{(33)}$$

The mass matrix for nine degrees of freedom per node is:

$$[m]_{9\times 9} = \begin{bmatrix} I_1 & & & & & & & & 0 \\ & I_1 & & & & & & & \\ & & I_1 & & & & & & \\ & & & I_2 & & & & & \\ & & & & I_2 & & & & \\ & & & & & I_3 & & & \\ & & & & & & I_3 & & \\ & & & & & & & I_4 & \\ 0 & & & & & & & & I_4 \end{bmatrix} \quad \textbf{(34)}$$

For layered plates, the element mass matrix can be written as follows:

$$[M] = \sum_{L=1}^{NL} [M]^e \quad \textbf{(35)}$$

where in the above Equation (34), I_1, I_2, I_3, and I_4 are translation inertia, rotary inertia, and respectively higher order inertia terms, and these are given by:

$$(I_1, I_2, I_3, I_4) = \sum_{L=1}^{NL} \int_{h_{L-1}}^{h_L} (1, z^2, z^4, z^6) \rho^L dz \quad \textbf{(36)}$$

where ρ^L is material density of L-th layer.

Formulation of Damping Properties

The most common form for the representation of the damping matrix [C] is the so-called Rayleigh-type damping [**Timoshenko** and **Gere**, **1961**][20] which was given as;

$$[C] = a_o [M] + a_1 [K] \quad \textbf{(37)}$$

in which (a_o and a_1) are arbitrary proportionality factors, which make the damping matrix satisfy the orthogonality condition with respect to the modal matrix [Φ] in the same way of the orthogonality conditions for the mass and stiffness matrices that is [**Bathe**, **1996**][17]:

$$\{\Phi\}^T [M]\{\Phi\} = [I]$$
$$\{\Phi\}^T [K]\{\Phi\} = [\Lambda] \quad \textbf{(38)}$$
$$\{\Phi\}^T [C]\{\Phi\} = 2[\gamma][\Lambda]^{1/2}$$

where

$\{\Phi\}$**:** The modal matrix whose columns represent the natural modal shapes and the superscript (T) denotes transpose.

$[I]$**:** Identity matrix.

$[\Lambda]$**:** Spectral matrix, which is a diagonal matrix with elements representing the squares of the natural frequencies (ω_i^2).

$[\gamma]$**:** Modal damping matrix which is also a diagonal matrix with elements representing the damping ratios for the system modes (γ_i)

Premultiplying Equation (37) by $\{\Phi\}^T$ and postmultiplying it by $\{\Phi\}$ yields :

$$\{\Phi\}^T [C]\{\Phi\} = a_o \{\Phi\}^T [M]\{\Phi\} + a_1 \{\Phi\}^T [K]\{\Phi\} \quad \textbf{(39)}$$

Substituting Equations (38) into Equation (39) gives;

$$2[\gamma][\Lambda]^{1/2} = a_o [I] + a_1 [\Lambda] \quad \textbf{(40)}$$

The two factors, a_o and a_1 can be determined by specifying the damping ratios for two modes for example 1 and 2, and substituting into Equation (40) as [**Pytet**, **1990**][18]:

$$2\gamma_1\omega_1 = a_o + a_1\omega_1^2 \quad \textbf{(41)}$$

$$2\gamma_2\omega_2 = a_o + a_1\omega_2^2 \quad \textbf{(42)}$$

where ω_1 and ω_2 are the natural frequencies for modes 1 and 2 respectively. By solving the above two Equations one can get:

$$a_o = \frac{2\omega_1\omega_2(\omega_2\gamma_1 - \omega_1\gamma_2)}{(\omega_2^2 - \omega_1^2)} \quad \textbf{(43)}$$

$$a_1 = \frac{2(\omega_2\gamma_2 - \omega_1\gamma_1)}{(\omega_2^2 - \omega_1^2)} \quad \textbf{(44)}$$

Then, the values of a_o and a_1 are substituted into Equation (37) to get the required damping matrix.

Failure criteria for laminated plate structure

The stresses in an individual lamina are fundamental to control the failure initiation and progression in the laminate. The strength of each individual lamina is assessed separately by considering the stresses acting on it along the material axes. The initial failure of a lamina is governed by exceeding the maximum limit prescribed by a failure criterion. The determination of failure load is very essential in understanding the failure process as well as the reliability and safety of structures. The ultimate load that makes the plate fail is calculated based on **Tsai-Wu** criterion for general composite materials and on **Hashin** criterion for fiber composite materials as follows [**Jones**, **1999**][10]
:

$$F_i\sigma_i + F_{ij}\sigma_i\sigma_j = 1; \qquad i,j = 1,.....,6 \tag{45}$$

where F_i and F_{ij} are strength tensors of the second and fourth order respectively and the usual contracted tensor notation is used except that $\sigma_4 = \tau_{13}, \sigma_5 = \tau_{23},$ and $\sigma_6 = \tau_{12}$. Equation (45) is obviously very complicated thus it will restrict the above attention to the reduction of above equation for an orthotropic lamina under plane stress conditions:

$$\begin{aligned} &F_1\sigma_1 + F_2\sigma_2 + F_3\sigma_3 + F_{11}\sigma_1^2 + +F_{22}\sigma_2^2 + F_{33}\sigma_3^2 + F_{12}\sigma_1\sigma_2 \\ &+ F_{13}\sigma_1\sigma_3 + F_{23}\sigma_2\sigma_3 + F_{44}\sigma_4^2 + F_{55}\sigma_5^2 + F_{66}\sigma_6^2 = 1 \end{aligned} \tag{46}$$

The terms that are linear in the stresses are useful in representing different strengths in tension and in compression. The terms that are quadratic in the stresses are the more or less usual terms to represent an ellipsoid in stress space, where $F_3 = 0$ indicates that to the shear strength of a material in compression and in tension is similar, and $\sigma_3 = 0$ in ***z***-direction. Also, the shear strength of a material is equal in three dimensions and equal to ***S***. Thus, the terms of F_i is:

$$\begin{aligned} &F_1 = \left(\frac{1}{X_t} - \frac{1}{X_c}\right), F_2 = \left(\frac{1}{Y_t} - \frac{1}{Y_c}\right), F_3 = \left(\frac{1}{Z_t} - \frac{1}{Z_c}\right) \\ &F_{11} = \left(\frac{1}{X_t.X_c}\right), F_{22} = \left(\frac{1}{Y_t.Y_c}\right), F_{33} = \left(\frac{1}{Z_t.Z_c}\right) \\ &F_{44} = \left(\frac{1}{R^2}\right), F_{55} = \left(\frac{1}{S^2}\right), F_{66} = \left(\frac{1}{T^2}\right) \\ &F_{12} = \frac{-1}{2}\left(\frac{1}{X_t.X_c.Y_tY_c}\right)^{0.5}, F_{13} = \frac{-1}{2}\left(\frac{1}{X_t.X_c.Z_c.Z_t}\right)^{0.5} \\ &F_{23} = \frac{-1}{2}\left(\frac{1}{Y_t.Y_c.Z_c.Z_t}\right)^{0.5} \end{aligned} \tag{47}$$

where,

$X_c, X_t =$ The axial or longitudinal strength in compression and tension.

$Y_c, Y_t =$ The transverse strength in compression and tension.

$Z_c, Z_t =$ The transverse strength in compression and tension.

$R, T, S =$ Shear strength of the material.

Equation (46) becomes as:

$$F_1\sigma_1 + F_2\sigma_2 + F_{11}\sigma_1^2 + +F_{22}\sigma_2^2 + F_{12}\sigma_1\sigma_2 + F_{44}\sigma_4^2 + F_{55}\sigma_5^2 + F_{66}\sigma_6^2 = 1 \qquad \textbf{(48)}$$

Equation (48) is suitable for the elastic-plastic analysis of anisotropic materials.

For matrix cracking failure, two different failure criteria are used depending on whether the transverse normal stress, σ_{22}, is in tension or in compression. The failure index, e_m^2, is defined in terms of transverse tensile strength, Y_t, transverse compressive strength, Y_c, and in-plane shear strength, R, and is expressed as:

$$e_m^2 = \frac{\sigma_{22}}{Y_c}\left[\left(\frac{Y_c}{2R}\right)^2 - 1\right] + \left(\frac{\sigma_{22}}{2R}\right)^2 + \left(\frac{\tau_{12}}{R}\right)^2 \quad \text{for } \sigma_{22} < 0 \qquad \textbf{(49)}$$

and,

$$e_m^2 = \left(\frac{\sigma_{22}}{Y_t}\right)^2 + \left(\frac{\tau_{12}}{R}\right)^2 \quad \text{for } \sigma_{22} > 0 \qquad \textbf{(50)}$$

where (e_m) is the failure index for matrix cracking. Matrix cracking is assumed to occur when the failure index (e_m) exceeds unity.

Fiber-matrix shear failure is assumed to be dependent on a combination of axial stress, σ_{11}, and shear stress, τ_{12}, and is expressed as follows:

$$e_s^2 = \left(\frac{\sigma_{11}}{X_t}\right)^2 + \left(\frac{\tau_{12}}{R}\right)^2 \quad \text{for } \sigma_{11} > 0 \text{ and } \left(\frac{\sigma_{11}}{X_t}\right)^2 < \left(\frac{\tau_{12}}{R}\right)^2 \qquad \textbf{(51)}$$

and,

$$e_s^2 = \left(\frac{\sigma_{11}}{X_c}\right)^2 + \left(\frac{\tau_{12}}{R}\right)^2 \quad \text{for } \sigma_{11} < 0 \text{ and } \left(\frac{\sigma_{11}}{X_t}\right)^2 < \left(\frac{\tau_{12}}{R}\right)^2 \qquad \textbf{(52)}$$

where (e_s) is the failure index for fiber-matrix shearing, X_t is the tensile strength along the fiber direction and X_c is the compressive strength along the fiber direction. Equations (51) and (52) predict that when the failure (e_s) exceeds unity, fiber-matrix shearing dominated failure occurs.

Fiber breakage failure occurs in tension due to the combination of axial stress and shear stress while the failure in compression is governed by buckling as expressed in terms of only axial stress. The criterion for breakage failure is expressed as follows:

$$e_f^2 = \left(\frac{\sigma_{11}}{X_t}\right)^2 + \left(\frac{\tau_{12}}{R}\right)^2 \quad \text{for } \sigma_{11} > 0 \qquad \textbf{(53)}$$

and,

$$e_f^2 = \left(\frac{\sigma_{11}}{X_c}\right)^{2^2} \quad \text{for } \sigma_{11} < 0 \qquad \textbf{(54)}$$

where (e_s) is the failure index for fiber breakage. The fiber breakage failure occurs when (e_s) exceeds unity.

Forced vibration analysis

The calculation of the nonlinear dynamic response of structure of structures including instability or buckling phenomena has received considerable attention and a good amount of literature has appeared on this subject. The nonlinear dynamic analysis depends largely on solving the following Equations:

$$[M]\{\ddot{d}(t)\}+[C]\{\dot{d}(t)\}+[K_T]\{d(t)\}=\{F(t)\} \qquad \textbf{(55)}$$

in which $[K_T]$ is the tangent stiffness matrix of the plate (or structure) and depends on the current displacements and stresses. The most conventional implicit time integration procedures is **Newmark** method. After solving Equation (55) at time ($t+\Delta t$) for displacements, velocities, and accelerations, the following equation as:

$$\begin{aligned}\left([K_T]+a_o[M]+a_1[C]\right)\{d\}_{t+\Delta t} = \{F(t)\}_{t+\Delta t} &+ [M]\left(a_2\{\dot{d}\}_t + a_3\{\ddot{d}\}_t\right) \\ &+ [C]\left(a_4\{\dot{d}\}_t + a_5\{\ddot{d}\}_t\right)\end{aligned} \qquad \textbf{(56)}$$

For convenience, the following is used:

$$[K_T]_{eff} = [K_T]+a_o[M]+a_1[C] \qquad \textbf{(57)}$$

and,

$$\{F(t)\}_{eff} = \{F(t)\}_{t+\Delta t} + [M]\left(a_2\{\dot{d}\}_t + a_3\{\ddot{d}\}_t\right)+[C]\left(a_4\{\dot{d}\}_t + a_5\{\ddot{d}\}_t\right) \qquad \textbf{(58)}$$

So, Equation (5.66) may be written in the form:

$$[K_T]_{eff}\{d\}_{t+\Delta t} = \{F(t)\}_{eff} \qquad \textbf{(59)}$$

For a linear system, $[K_T]_{eff}$ will be constant during the analysis at any time, while in the nonlinear analysis, $[K_T]_{eff}$ is a function of current displacement vector $\{d\}$. Therefore, an iterative procedure must be used to define $[K_T]_{eff}$. In the nonlinear analysis, it is more useful to put Equation (59) in increment form. For such purpose, Equation (59) may be rewritten as:

$$[\hat{K}_T]\{\Delta d\} = \{\Delta \hat{F}(t)\} \qquad \textbf{(60)}$$

in which $[\hat{K}_T]$ is the effective stiffness matrix and $\{\Delta \hat{F}(t)\}$ is the effective load vector. Equation (60) is solved by an iterative procedure like Equation (56). It may be noted that Equation (56) may be used for solving linear problems, while for nonlinear problems, Equation (60) should be used.

Solving Equation (60) for $\{\Delta d\}$, approximate values for accelerations, velocities and displacements may be given as:

$$\begin{aligned}
\{\ddot{d}\}_{t+\Delta t} &= a_o\{\Delta d\} - a_2\{\dot{d}\}_t - a_3\{\ddot{d}\}_t \\
\{\dot{d}\}_{t+\Delta t} &= a_1\{\Delta d\} - a_4\{\dot{d}\}_t - a_5\{\ddot{d}\}_t \\
\{d\}_{t+\Delta t} &= \{d\}_t + \{\Delta d\}\ ;
\end{aligned} \qquad \textbf{(61)}$$

Where

$$a_o = \frac{1}{\beta(\Delta t)^2},\ a_1 = \frac{\gamma}{\beta(\Delta t)},\ a_2 = \frac{1}{\beta(\Delta t)},\ a_3 = \frac{1}{2\beta} - 1$$

$$a_4 = \frac{\gamma}{\beta} - 1,\ a_5 = \frac{\Delta t}{2}\left(\frac{\gamma}{\beta} - 2\right)$$

Applications and Discussions

Several plates are analyzed to study the different effects on the large displacement elastic-plastic dynamic behavior of plates with some comparison with other researchers.

Comparison with available theoretical investigation of composite plate

Clamped supported square angle-ply laminated plate under transverse suddenly applied constant dynamic loading

A square angle-ply ($0^o/45^o/90^o$/core/$90^o/45^o/30^o/0^o$) sandwich laminated plate with clamped edges and subjected to a suddenly applied uniformly transverse load was analyzed and compared with **Kommineni** and **Kant** [**1993**][14]. The following layer material properties are used in the analysis: for face sheets (Graphite/epoxy prereg system) (E_1=130.8 GPa; E_2=10.6 GPa G_{12}=G_{13}=6 GPa; G_{23}=3.9 GPa; ν_{12}=0.28; and ρ=15.8 kN.sec^2/m^4); for core sheet (US Commercial al. honeycomb, ¼ in cell size, 0.003 in foil) (G_{13}=0.5206 GPa; G_{23}=0.1772 GPa; ρ=1.009 kN.sec^2/m^4). The time step is (Δt=0.000025 sec),and applied load (q=50 kN/m^2). The geometry properties are (a=1.0 m, a/b=1, and h=0.01m, at top three stiff layers, thickness of each layer=0.025 h, at bottom four stiff layer, thickness of each layer=0.08125 h, and thickness of core=0.6 h). **Kommineni** and **Kant** used nine-node isoparametric Lagrangian elements with nine-node degrees of freedom per node and divided the full plate into (4×4) element mesh.

In the present study, the full laminated plate is modeled by (4×4) element mesh with nine-node isoparametric Lagrangian element and nine degrees of freedom per node. A consistent mass matrix and **Newmark** integration method with α=1/2, and β=1/4 were used in the present study.

Figure (6) shows the time history curve for the clamped angle-ply laminated plate under transverse suddenly applied load. From this figure, it can be noticed that good agreement with other study exists with a difference not exceeding (1%).

Parametric Study

To investigate the large displacement elastic-plastic dynamic behavior of laminated composite plate under in-plane dynamic loading, effects of several important parameters were studied.

The selected parametric studies can be summarized as follows:

1. The effect of through-thickness shear deformation.
2. The effect of fiber's orientation angle.
3. The effect of damping.
4. The effect of fiber waviness.

Each one of the above parameters was studied individually by analyzing a type of laminated composite plate. In all cases, the nine-node isoparametric Lagrangian element was used and one quadrant of the plate was analyzed due to symmetry and (2×2) element mesh which was used for the cross-ply laminated plates while the angle-ply and sine wave fiber plates were analyzed by considering full plates with (4×4) element mesh. The following geometry and layer material properties of high graphite epoxy are used in the analysis: (E_1=172.5 GPa; E_2=7.08 GPa; G_{12}=G_{13}=3.45 GPa, G_{23}=1.38 GPa; E_f=341.42 GPa; E_m=3.58 GPa; V_f=0.5; V_m=0.5; ν_{12}=ν_{13}=ν_{23}=0.25, ρ=15.8 kN.sec^2/m^4 X_t=X_c=1450 MPa, Y_t=36 MPa, Y_c=230 MPa, S=62 MPa)[83]. The geometry properties are (a=1.0 m, a/b=1).

1. Effect of through-thickness shear deformation

To study the effect of shear deformation on the large displacement elastic-plastic dynamic analysis of a laminated composite plate under in-plane constant dynamic loading, a simply supported square plate with slenderness ratio (b/h=20), and with symmetric cross-ply and antisymmetric cross-ply arrangements and with eight layers was analyzed. The initial imperfection is (w_o/h= 0.1) by which the shape is considered to be a sinusoidal curve.

Figures (7) and (8) present the time history curves for the symmetric cross-ply, and for the antisymmetric cross-ply laminated composite plates by taking the through-thickness shear deformation through the degrees of freedom of the element. From these figures, it can be noticed that increasing the number of degrees of freedom per node from five degrees to nine degrees will increase the central deflection about (16%) for symmetric cross-ply and about (20%) for antisymmetric cross-ply plates.

2.Effect of fiber's orientation angle

To show the effect of fiber's orientation angle on the large displacement elastic-plastic dynamic analysis of laminated composite plates under in-plane constant dynamic loading, a simply supported square plate with slenderness ratio (b/h=60) was considered. The initial imperfection was (w_o/h= 0.1) by which the shape was considered to be a sinusoidal curve. A consistent mass matrix and **Newmark**

integration method with α=1/2, and β=1/4 were used in the present study. A quarter of the laminated plate was modeled (2×2) element mesh with nine-node isoparametric Lagrangian elements having nine degrees of freedom per node.

Figure (9) presents the time history curve for the laminated simply supported square plate under in-plane dynamic loading and with many types of fiber's orientation angle. From this figure, it could be noticed that the central deflection of the plate with ($0^o/90^o$) is less than the deflections of others, this orientation's fiber is the optimum for a plate under in-plane dynamic loading.

3. Effect of damping

To study the effect of damping on the large displacement elastic-plastic dynamic behavior of composite plates, two examples are considered. The first one is a simply supported square plate with symmetric cross-ply lamination with eight layers and under in-plane dynamic

loading. The second one is a simply supported square plate with antisymmetric cross-ply lamination with eight layers and under in-plane dynamic loading. Different values of damping factor (0.0-0.1) are considered in the present study. The initial imperfection shape is considered to be a sinusoidal curve.A quarter of the laminated plate is modeled by (2×2) element mesh with nine-node isoparametric Lagrangian elements having nine degrees of freedom per node. The plates were analyzed under in-plane constant dynamic loading ratio (P_x/P_u=0.65) for the symmetric cross-ply plate and (P_x/P_u=0.6) for the antisymmetric cross-ply plate.

Figure (10) presents the time history curve for a simply supported square plate with symmetric cross-ply lamination under in-plane constant loading with a range of damping factor (γ) (0.0-0.1).

Figure (11) presents the time history curve for a simply supported square plate with antisymmetric cross-ply lamination under in-plane constant loading with range of damping factor (γ) (0.0-0.1). It is noticed that the response (deflection) decreases with the increase of the damping factor. Also, the plate shows no oscillation about the static deflection position for damping factors greater than or equal to (0.05). This means that the plate is under the critical damping ratio. So, it can be seen that the antisymmetric lamination of plates has a rate of damping faster than symmetric lamination. This type of lamination can be used in places that need damping property

.

4. Effect of fiber waviness

To study the effect of fiber waviness on the large displacement elastic-plastic dynamic behavior of composite (laminated) plate, two types of lamination were considered. The first one is a simply supported square plate, laminated plate with eight layers under in-plane constant dynamic loading. The second one is a simply supported square symmetric cross-ply laminated plate with eight layers under also constant dynamic loading. Different values of fiber path amplitude (Δ) (0.05-0.5) and different numbers of sequences (k) (4-12) were considered. The plates were under in-plane constant dynamic loading (250 kN/m). In the present study, the full laminate plate

was modeled with (4×4) element mesh with nine-node isoprametric Lagrangian elements having nine degrees of freedom per node. A consistent mass matrix and **Newmark** integration method with α=1/2, and β=1/4 were used in the present study.

Figures (12)-(14) show the time history curves for the simply supported composite laminated plate with eight layers having sine wave fiber $(0)_8$ and under in-plane constant dynamic loading.

Figures (15)-(17) show the time history curves for the square symmetric cross-ply composite laminated plate under in-plane suddenly applied constant dynamic loading and having eight layers with sine wave fiber.

From these figures, the following can be noticed:

1. The oscillation of the symmetric cross-ply laminated composite plate with sine wave fiber ($\boldsymbol{k}$=12,Δ=0.4) is less than that of other plates.
2. The time capacity of the laminated plate with symmetric cross-ply lamination and with sine wave fiber ($\boldsymbol{k}$=4 and $\boldsymbol{k}$=12) is greater than the time capacity of the laminated plate with symmetric cross-ply lamination and with sine wave fiber ($\boldsymbol{k}$=8).
3. The time capacity of the laminated plate with sine wave fiber ($\boldsymbol{k}$=8,Δ=0.4) is greater than that of the others and also the time capacity of the symmetric cross-ply plate with sine wave fiber ($\boldsymbol{k}$=8,Δ=0.2) is greater than that of the others.

Conclusions

A nonlinear finite element method is adopted for the large displacement elastic-plastic dynamic analysis of anisotropic plates under in-plane compressive load. Damping property is considered by using Rayleigh type damping which is linearly related to the mass and the stiffness matrices. **Newmark** integration method is used for solving the dynamic equilibrium equations. The effects of initial imperfection, orthotropy of individual layers, fiber's orientation angle, type of loading, damping factor, and fiber waviness on the large displacement elastic-plastic dynamic analysis are considered. The conclusion it is shown that the antisymmetric cross-ply laminated plate has a damping rate faster than the symmetric cross-ply laminated plate and if damping is considered and if the response of the plate shows no oscillation about the static deflection position, it means that the damping factor is below the critical damping factor.

References

1. Abid-Ali, A. K., "Stress Analysis of Laminated Fiber Reinforced Composite Cylinder", M.Sc. Thesis, University of Babylon, Hilla, Iraq, 2000.
2. Ali, A. A., "Vibration and Stability Analysis of Frame-Type Structures and Plates Using Beam-Column Analogy", PhD. Thesis, University of Technology, Building and Construction Department, Baghdad, Iraq, 2004.
3. Ali, N. H., "Finite Element Dynamic Analysis of Laminated Composite Plates Including Damping Effect", M.Sc. Thesis, University of Babylon, Hilla, Iraq, 2004.

4. Akay, H. "Dynamic Large Deformation Analysis of Plates Using Mixed Finite Elements" Comp. & Struct., Vol.11, 1980, pp1-11.
5. Amash, H. K., "Nonlinear Static and Dynamic Analysis of Laminated Plates Under In-plane Forces", Ph.D. Thesis, University of Babylon, Hilla, Iraq, 2008.
6. Azevedo, R.L. and Awruch, A.M. "Geometric Nonlinear Dynamic Analysis of Plates and Shells Using Eight-Node Hexahedral Finite Element with Reduced Integration", J. Braz. Soc. Mech. Sci., Vol.21, No.3, 1999, pp.1-22.
7. Bathe, K.J., and Ozdemir, H. "Elastic-Plastic Large Deformation Static and Dynamic Analysis.", Comp. & Struct., Vol.6, No.2, 1975, pp81-92.
8. Cook, R.D., "Finite Element Modeling for Stress Analysis", John Wiley & Sons, Inc., 1995.
9. Hashin, Z. "Failure Criteria for Unidirectional Fiber Composites", ASME, J. Appl. Mech., Vol.47, 1980, pp.329-334.
10. Jones, R.M., "Mechanics of Composite Materials", Second Edition, Taylor and Francis Inc., U.S.A., 1999.
11. Kao, R., "Nonlinear Dyanmic Buckling of Spherical Caps with Initial Imperfections", Comp. & Struct., Vol.12, 1980, pp49-63.
12. Kaw, A., "Mechanics of Composite Materials", Second Edition, Taylor and Francis Group, LLC, 2006.
13. Khante, S. N., Rode, V., and Kant, T., "Nonlinear Transient Dynamic Response of Damping Plates Using a Higher Order Shear Deformation Theory", Nonlinear Dynamics, Vol.47, 2007, pp38-403.
14. Kommineni, J. R., and Kant, T. "Geometrically Non-linear Transient C^o Finite Element Analysis of Composite and Sandwich Plates with a Refined Theory." Struct. Eng. And Mech., Vol.1, No.1, 1993, pp87-102.
15. Pandey, M. D., "Effect of Fiber Waviness on Buckling Strength of Composite Plates." ASCE, J. Eng. Mech., Vol.125, No.10, 1999, pp.1173-1179.
16. Parhi, P.K., Bhattacharyya, S.K., and Sinha, P.K. "Failure Analysis of Multiple Delaminated Composite Plates Due to Bending and Impact" Bull. Mater. Sci., Vol.24, No.2, 2001, pp143-149.
17. Pica, A., Wood, R.D., and Hinton, E. "Finite Element Analysis of Geometrically Nonlinear Plate Behavior Using a Mindlin Formulation." Comp. & Struct., Vol.11, 1979, pp.203-215.
18. Pytet, M., "Introduction to Finite Element Vibration Analysis", 1990.
19. Tao, Z., Tu-guang, L., Yao,Z., and Jio-zhi,L. "Nonlinear Dynamic Buckling of Stiffened Plates under In-plane Impact Load.", J. Zhejiang University Science, Vol.5, No.5, 2004, pp609-617.
20. Timoshenko, S.P., and Gere, J.M., "Theory of Elastic Stability", 2nd Ed, McGraw-Hill Book Co., Inc., New York, 1961.
21. Weller, T., Abramovich, H., and Yaffe, R., "Dynamic Buckling of Beams and Plates Subjected to Axial Impact", Comp. & Struct., Vol.32, No.3/4, 1989, pp835-851.

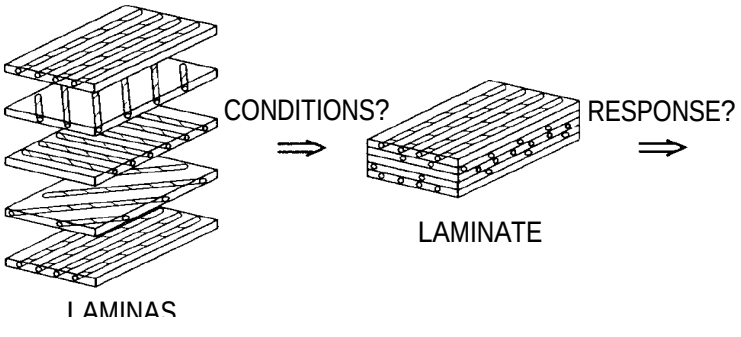

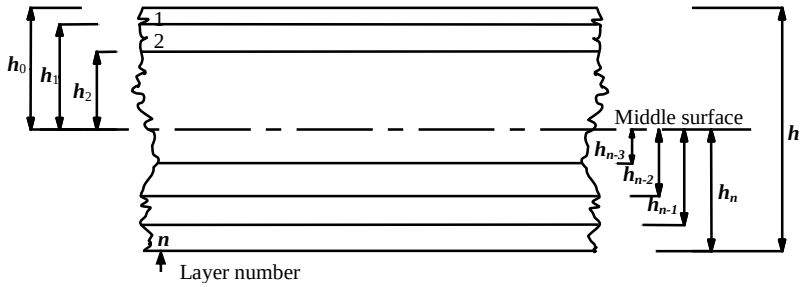

Figure (2): Geometry of an NL-layered laminate [**Jones**,**1999**][10]

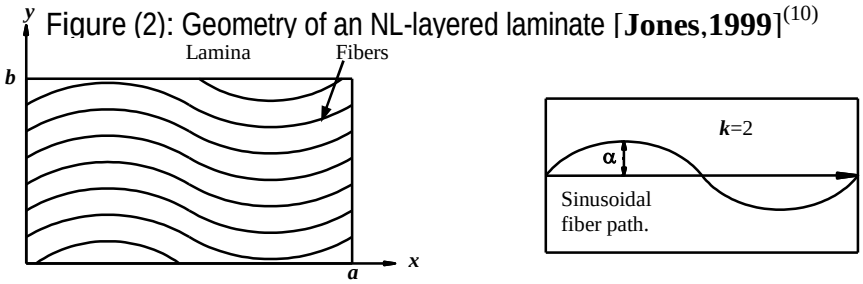

(a) (b)

Fiber (3): (a) Lamina with variable fiber orientation; (b) Geometry of sinusoidal fiber path [**Pandey**,**1999**][15]

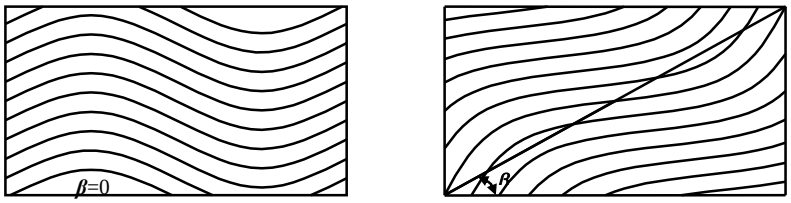

Figure (4): Laminate plate with sine wave fibers aligned with ***x***-axis

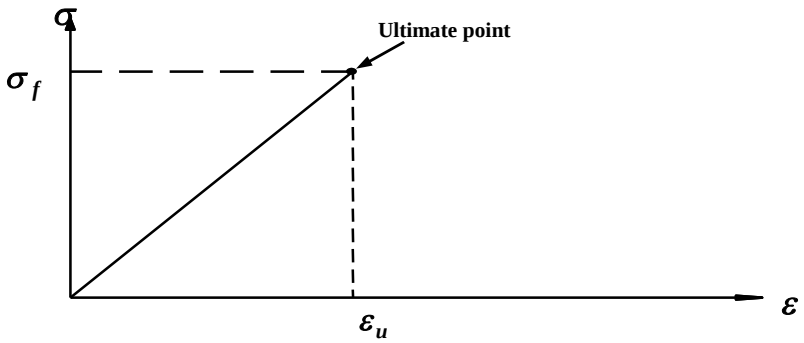

Figure (5): Idealizated stress-strain relationship of uniaxial loading behavior for orthrotropic plate[**Jones, 1999**][10]

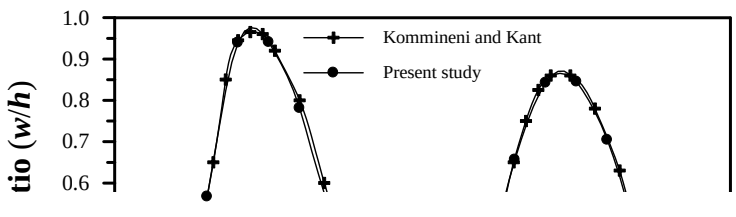

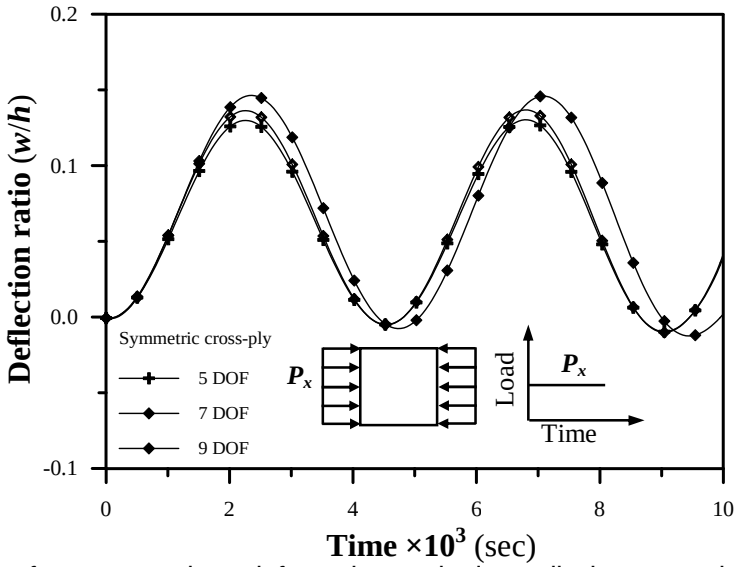

Figure (7): Effect of transverse shear deformation on the large displacement elastic-plastic analysis of symmetric cross-ply laminated plate under in-plane constant dynamic loading ratio (P_x/P_u=0.3), (b/h=20,Δt=0.0001, w_o/h=0.1,P_u=18563 kN/m)

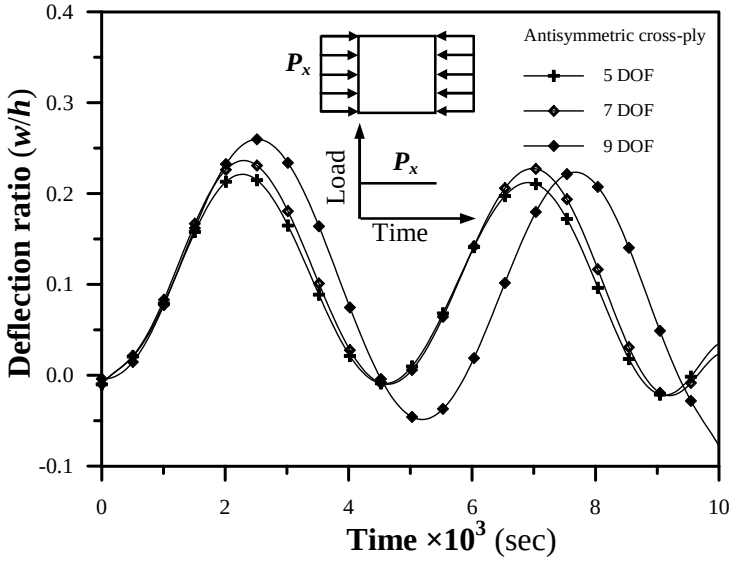

Figure (8): Effect of transverse shear deformation on the large displacement elastic-plastic analysis of antisymmetric cross-ply laminated plate under in-plane constant dynamic loading ratio (P_x/P_u=0.3),

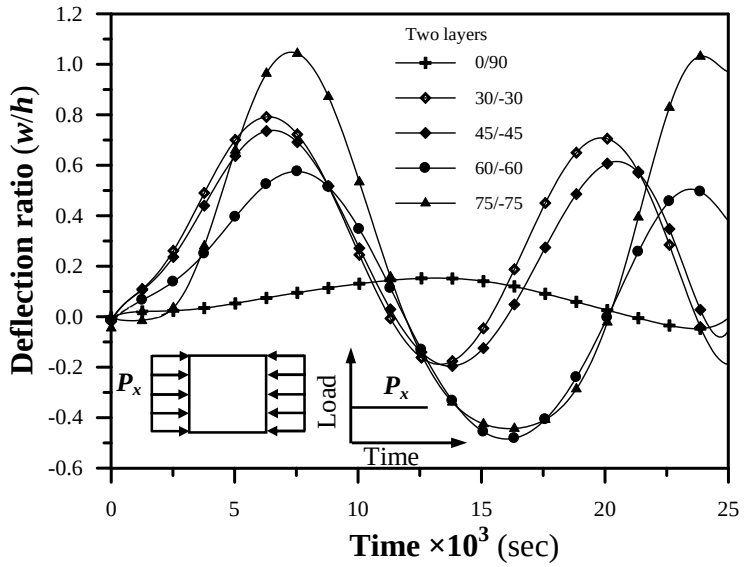

Figure (9): Effect of fiber's orientation angle on the large displacement elastic-plastic analysis of a laminated simply supported square plate under in-plane constant dynamic loading (P_x=700 kN/m), (b/h=60, Δt=0.0001, w_o/h=0.1)

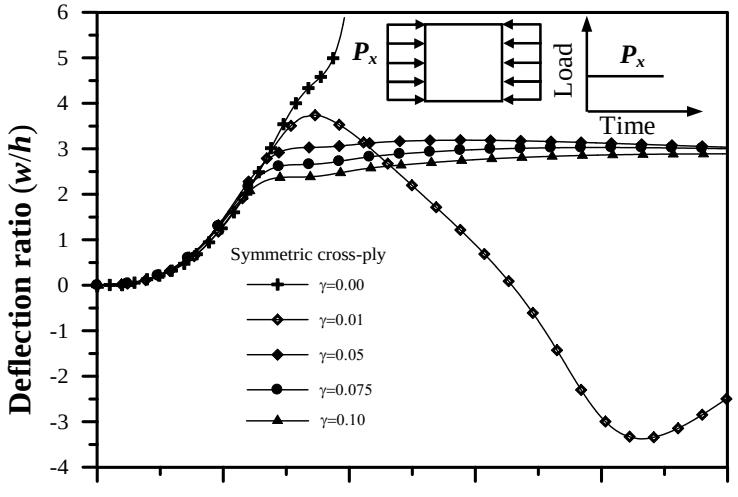

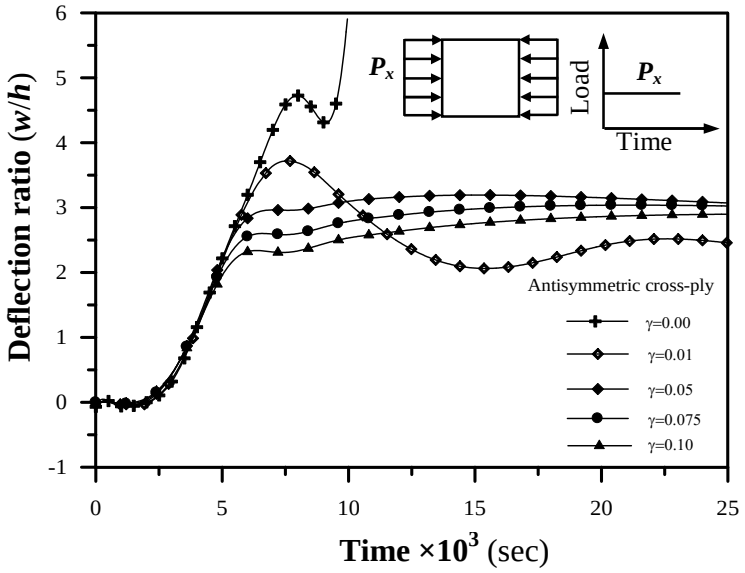

Figure (11): Effect of damping factor on the large displacement elastic-plastic analysis of a simply supported square antisymmetric cross-ply plate under in-plane constant dynamic loading, (b/h=100, Δt=0.0001, w_o/h=0.1, P_x/P_u=0.60)

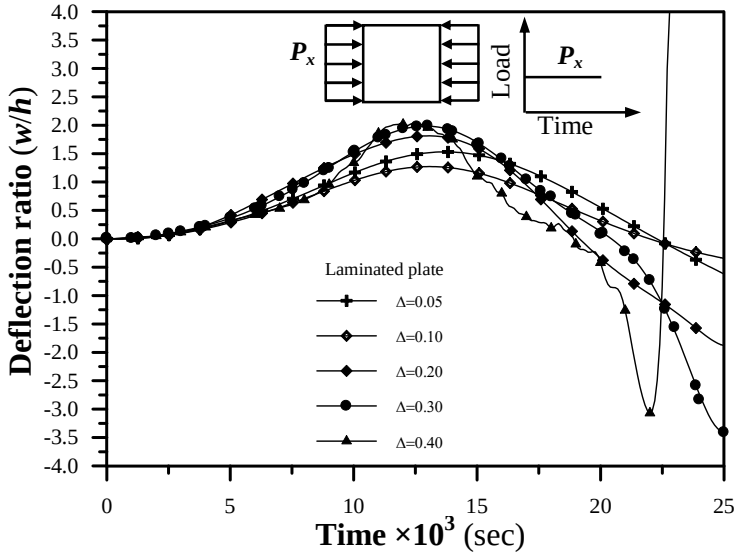

Figure (12): Effect of fiber waviness on the large displacement elastic-plastic analysis of a simply supported square laminated plate under in-plane constant dynamic loading, (b/h=100, Δt=0.0001

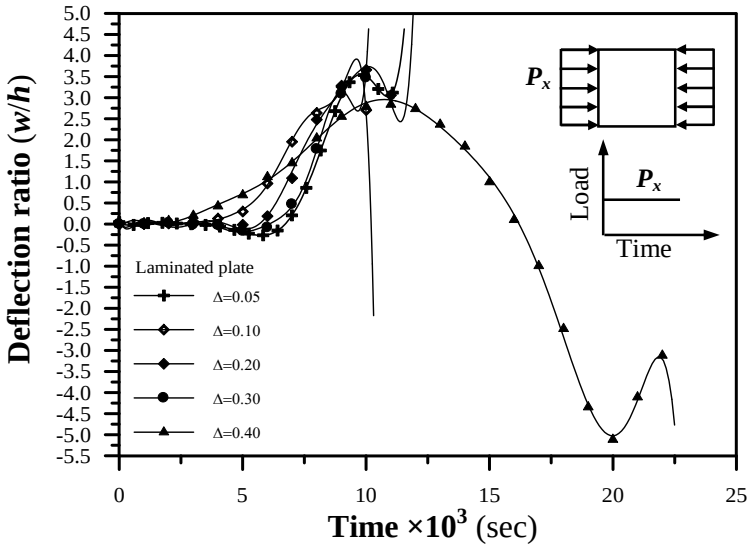

Figure (13): Effect of fiber waviness on the large displacement elastic-plastic analysis of a simply supported square laminated plate under in-plane constant dynamic loading, (b/h=100, Δt=0.0001, w_o/h=0.1, P_x=250 kN/m, k=8)

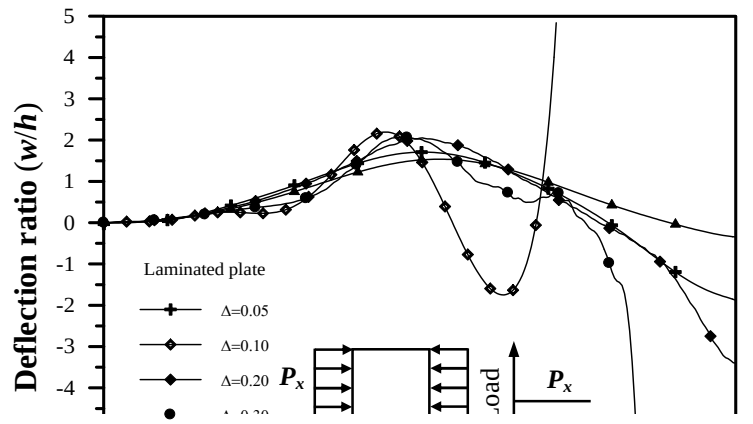

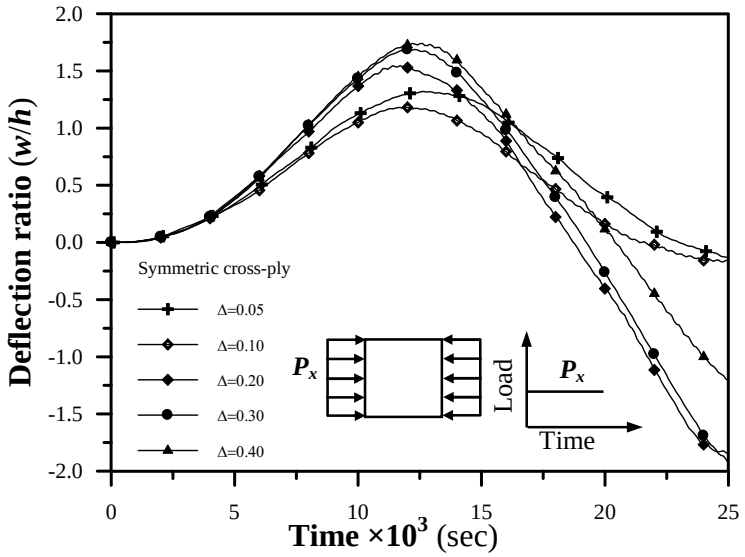

Figure (15): Effect of fiber waviness on the large displacement elastic-plastic analysis of a simply supported square symmetric cross-ply plate under in-plane constant dynamic loading, (b/h=100, Δt=0.0001, w_o/h=0.1, P_x=250 kN/m, k=4)

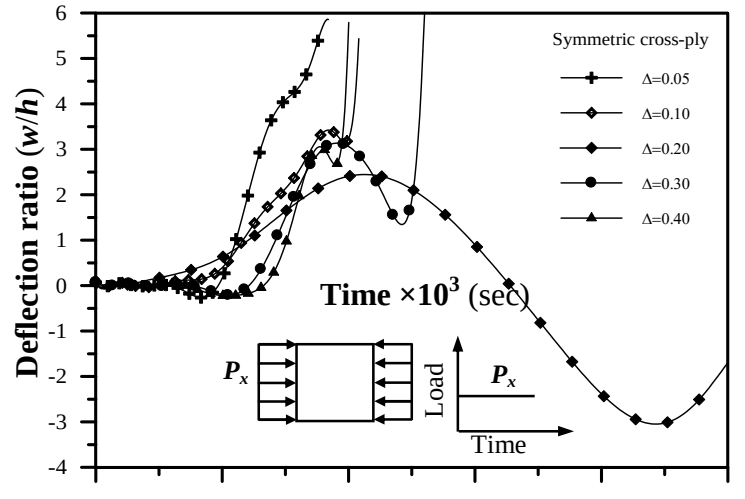

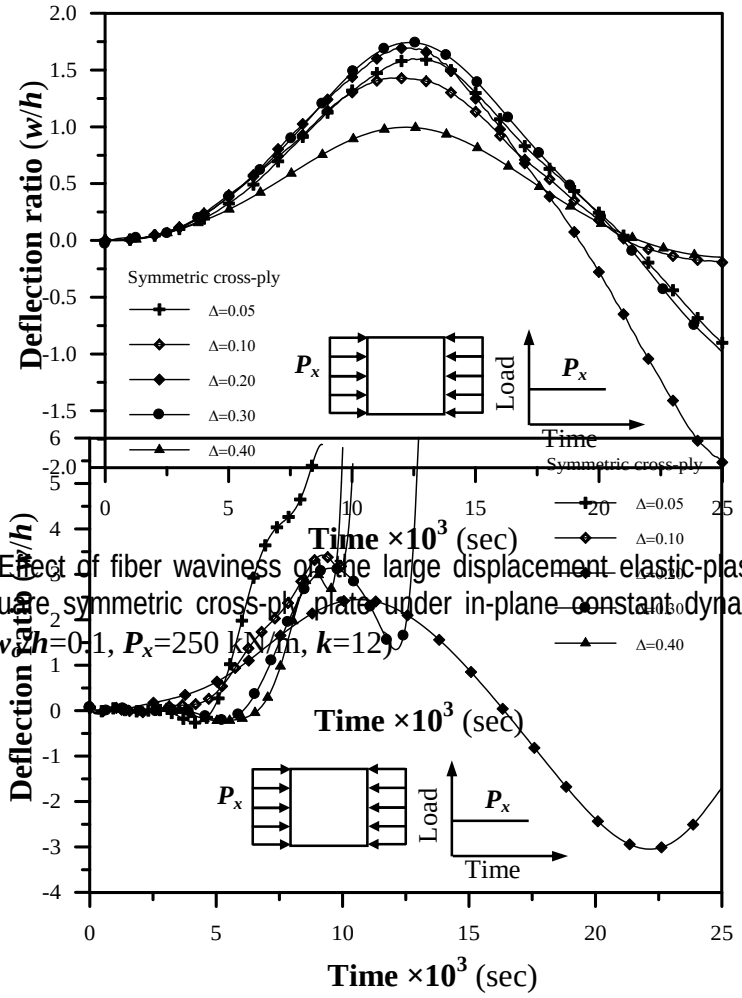

Figure (17): Effect of fiber waviness on the large displacement elastic-plastic analysis of a simply supported square symmetric cross-ply plate under in-plane constant dynamic loading, (***b/h***=100, **Δ*t***=0.0001, ***w*_o/h**=0.1, ***P*_x**=250 kN/m, ***k***=12)

Figure (16): Effect of fiber waviness on the large displacement elastic-plastic analysis of a simply supported square symmetric cross-ply plate under in-plane constant dynamic loading, (***b/h***=100, **Δ*t***=0.0001, ***w*_o/h**=0.1, ***P*_x**=250 kN/m, ***k***=8)